Evaluation of Power Capacity Availability at Load Bus in a Composite Power System

T. Bharath Kumar, O. Chandra Sekhar, M. Ramamoorty, *Life Fellow, IEEE*, and S. V. N. L. Lalitha, *Senior Member, IEEE*

***Abstract*— The evaluation of reliability of a composite power system is essential for the modern power system to assess the capacity to supply continuous power to the consumers. The power system network is affected by various uncertainties such as equipment failures and random variations in power generation and load demand. All these factors and complex network topology with a large number of equipment components lead to difficulties in the assessment of reliability in a composite power system. In this paper, reliability evaluation is carried out to estimate the power capacity availability at load bus in a composite power system. The composite power system considered here is a microgrid consisting of a conventional power generating unit, power transformer, wind farm, and four loads. New simplified predictive models have been suggested for the estimation of ambient temperature and wind velocity and validated with the actual weather data collected from Meteorological and Oceanographic Satellite Data Archival Centre, India. Using these models, wind velocity and ambient temperatures are predicted one day ahead to estimate the transformer tank temperature, from which the transformer derating factor and the power injected into the microgrid are computed. The proposed methodology is aimed to obtain the power capacity availability at load bus, the limits on the available power capacity variation, and corresponding confidence limits.**

***Index Terms*— Availability, composite power system, failure rate (λ), reliability, repair rate (μ).**

I. Introduction

THE electrical energy plays a vital role in our day-to-day life to meet the needs of modern society. The reliability evaluation of the electrical system is important to assess the quality of power system. The power system operators must aim to provide continuous power supply to the consumers at a reasonable cost. The reliability and probability evaluation methods for the power system are developed in [1]–[3]. The reliability assessment based on probability of available power capacity at load bus in an interconnected system is quite difficult due to the large number of equipment components, network topology, and constraints on its generation capacity [4]–[7].

The power transformer is one of the most important equipment components of electrical transmission and distribution systems. The capital investment of the power transformer is high compared with that of the other elements in transmission and distribution substations. Periodical maintenance and continuous monitoring is important for power transformers for better operation. Failures of power transformers lead to financial loss and replacement cost and require large downtime. A complete power outage will occur in the associate transmission and distribution systems due to power transformer failures. Hence, estimation of service life of power transformers is a well-known topic of interest [11]–[23]. Overloading of the power transformers is common and can occur in different forms such as continuous and intermittent due to various factors such as planned or emergency contingencies. The failure may be due to overloading, so the prediction of available transformer capacity is required to control the load. Derating of the transformer based on the harmonics and unbalanced and overloading conditions has been presented by Kumar *et al.* [29], Kolar *et al.* [30], Boroyevich *et al.* [31], Han *et al.* [32], and Fatu *et al.* [33] . Some of the recent developments in the microgrid are available in [29]–[33].

All these factors affect the power availability at the load bus. The reliability estimation in composite system is helpful to power system planners to take decisions on creating redundancy. This paper presents the methodology for evaluating the power capacity availability at load bus. It also provides knowledge in advance about some idea on the confidence level with which the available power capacity changes, which will be helpful to both the consumers and power system operators.

The following sections describe the procedure adopted for the available power capacity evaluation. Section II deals with the composite power system reliability and its importance. Section III discusses the methodology used for assessing the available capacity of power transformer through the calculation of its tank temperature based on the prediction of wind velocity and ambient temperature and evaluation of transformer derating factor based on the tank temperature. The evaluation of available power capacity at load bus is discussed in Section IV. Sections V and VI deal with the results and the conclusion, respectively.

II. Composite Power System

The reliability assessment is very important for the power system operation and control. The evaluation of reliability in the composite system is complex in nature due to the large number of equipment components and network topology. This is a challenging issue in the reliability evaluation in

Manuscript received February 13, 2016; revised June 16, 2016 and September 12, 2016; accepted October 3, 2016. Date of publication October 8, 2016; date of current version October 28, 2016. Recommended for publication by Associate Editor Liuchen Chang.

The authors are with the Electrical and Electronics Engineering, K L University, Vijayawada 522502, India (e-mail: tbkumar256@kluniversity.in; sekharobbu@kluniversity.in; mrmoorty@gmail.com; lalitha@kluniversity.in).

Color versions of one or more of the figures in this paper are available online at http://ieeexplore.ieee.org.

Digital Object Identifier 10.1109/JESTPE.2016.2615655

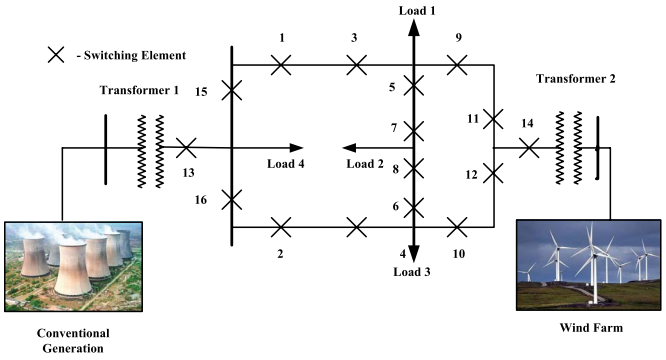

Fig. 1. Microgrid.

TABLE I
COMPOSITE POWER SYSTEM DATA

Component	Failure Rate λ (Fails/Yr)	Repair Rate μ (Repairs/Yr)
C.B 1	0.1	20
2	0.3	10
3	0.2	30
4	0.6	40
5	0.5	20
6	0.2	10
7	0.4	10
8	0.1	20
9	0.3	40
10	0.2	10
11	0.3	30
12	0.4	10
13	0.5	20
14	0.1	40
15	0.2	30
16	0.4	10
Conventional & Wind Generator	0.1	10
Power Transformer 1& 2	0.1	10

interconnected power systems [5]. The increased complexity of systems, competitive costs, types of designs, loss of revenue due to interrupted supply, and lack of periodical maintenance procedures are the main reasons that affect the reliability in the composite power system. The proposed composite power system is a microgrid consisting of a conventional generating unit of rating 5 MVA, two power transformers, wind farm of rating 5 MVA, and four loads as shown in Fig. 1. The failure and repair rates of each component are given in Table I. The nominal ratings of power transformers are the same as those of their connected generators. The wind power generation is fixed at 5 MVA irrespective of wind velocities above the rated value.

III. POWER CAPACITY AVAILABILITY

An interconnected power system consists of a number of equipment components that have their own failure and repair rates. The reliability index considered here is the power availability at load bus. The system considered here is a microgrid with a wind farm and a conventional generating unit as shown in Fig. 1. The most commonly used methods are series–parallel and star–delta conversions of the reliability model of the network using the individual failure and repair rates of each component and then from the power flow paths and so on. From this analysis, an equivalent failure (λ) and repair (μ) rates are obtained between the source and the load [28]. Once the failure and repair rates are computed, then the average power availability is calculated from (1) and (2). The classical node elimination method, which simplifies the analysis, is applied here to get the equivalent failure and repair rates and is explained in [28]

$$\text{Availability} = \frac{\mu}{(\lambda+\mu)} \tag{1}$$

$$\text{Unavailability} = \frac{\lambda}{(\lambda+\mu)}. \tag{2}$$

A. Prediction of Wind Velocity, Ambient Temperature, and Tank Temperature

In this paper, hourly metrological data of the past one week are collected from Meteorological and Oceanographic Satellite Data Archival Centre (MOSDAC) to predict the wind velocity, tank temperature, and ambient temperature for the eighth day. In general, the tank temperature is high compared with ambient temperature. This is because of the heat dissipation from the tank to ambient. The heat transfer is mainly due to convection [8]–[17]. From the MOSADC data, it is observed that if the ambient temperature and wind velocity are high, then the difference between the ambient and tank temperatures is less. Similarly, it is observed if the ambient temperature is high and wind velocity is low, then the difference between the ambient and tank temperatures is high [18]–[23]. This is due to the convective heat loss from the tank, which depends on both ambient temperature and wind velocity. That means there is a correlation among the wind velocity, tank temperature, and ambient temperature [24]–[27]. It is also observed that the wind velocity has a greater influence on the tank temperature. It is therefore necessary for the estimation of the tank temperature, wind velocity, and ambient temperature to be monitored near the transformer. However, the microgrid area under consideration is not very large and only one monitoring system for MOSADC data is located in that area, and an approximation is made that the wind velocity and ambient temperature are uniform in this region.

In order to predict the wind velocity on the eighth day based on the past seven-day hourly data. The hourly wind velocity V_n on any day is calculated from the weekly average wind velocity, V_o for the particular hour in the previous week, its standard deviation σ, and constant A_n, as given by

$$V_n = V_o + \sigma A_n. \tag{3}$$

Here, one-week hourly wind velocity is taken to compute the average wind velocity (V_o) and σ. The constant A_n for a particular hour of the day is assumed to follow a second-order polynomial as given in (4). The hourly based data of one-week wind velocity are shown in Table II

$$A_n = m_0 + m_1 X + m_2 X^2 \tag{4}$$

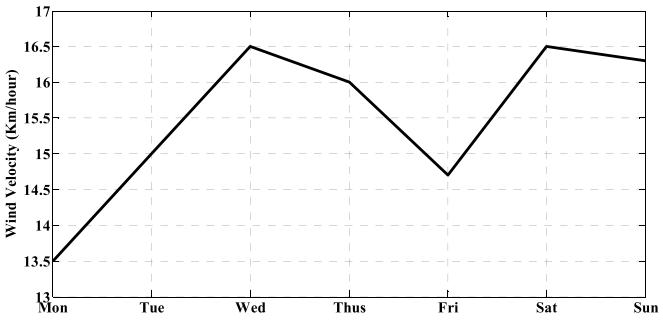

Fig. 2. Profile of wind velocity.

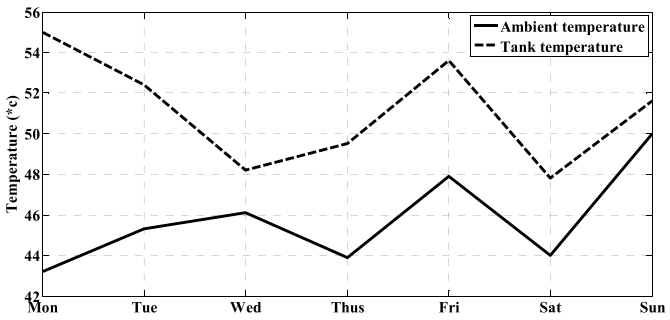

Fig. 3. Profile of ambient temperature and tank temperature.

TABLE II
VELOCITY, AMBIENT TEMPERATURE, AND TANK TEMPERATURE DATA FOR THE PAST ONE WEEK IN A PARTICULAR HOUR

S. No	Day	Wind Velocity (km/hour)	Ambient Temperature (°C)	Tank Temperature (°C)
1	Mon	13.5	43.2	55.0
2	Tue	15.0	45.3	52.4
3	Wed	16.5	46.1	48.2
4	Thus	16.0	43.9	49.5
5	Fri	14.7	47.9	53.6
6	Sat	16.5	44.0	47.8
7	Sun	16.3	50.0	51.2

where A_n = constant corresponds to the day number ($n = 1$ to 7), m_0, m_1, and m_2 are the constants, and X is the day number (1 to 7).

The profile of the wind velocity in a particular hour of the day for the past week is shown in Fig. 2. From the weekly wind data for the hour under consideration, the average wind velocity for the week and its standard deviation are calculated, and from (3), the constants A_1 to A_7 $((V_n - V_o)/\sigma)$ for the particular hour in the week are calculated. Using (4), constants m_0, m_1, and m_2 are evaluated by minimizing the square of the error in the calculation of A_n. From these data using the previously calculated constants m_0, m_1, and m_2, the wind velocity for the eighth day for the hour under consideration is computed. It is assumed that the average wind velocity and its standard deviation remain the same for the eighth day for the specified hour.

The predictions of wind velocity and ambient temperature through (3) and (4) are validated for the eighth day with the data collected from MOSDAC, Government of India, and the same is shown in Tables VIII–XI.

A similar procedure is used for predicting the ambient temperature for the eighth day based on the collected data available over the last week. The tank temperature and ambient temperature for the particular hour in the past week are also shown in Table II. The profile of these temperatures are plotted and shown in Fig. 3. The constants in (4) for each day are calculated and shown in Table III.

As stated earlier, the tank temperature depends on the wind velocity, ambient temperature, and the internal losses of the transformer. This relationship is given in the following :

$$\begin{aligned}\text{Tank temperature} = {} & (K_1 \times \text{Wind Velocity}) \\ & + (K_2 \times \text{Ambient temperature}) \\ & + K_0 \end{aligned} \tag{5}$$

where K_0 takes care of the variable load on the transformer

From the past one-week data, the variables K_1, K_2, and K_0 are determined to minimize the error between the measured and computed values of tank temperature. Using the constants K_1, K_2, and K_o and the predicted values of wind velocity and ambient temperature, the tank temperature for the eighth day for the particular hour is computed. Since the tank temperature is dependent on wind velocity and ambient temperature, which are varying with time, it is not correct to predict the tank temperature also from its past one-week data as is done for wind velocity and ambient temperature. Hence, the suggested procedure for estimating the tank temperature for the eighth day is followed.

Constants K_1, K_2, and K_0 in (5) are calculated from the past one-week data are $K_1 = -2.9909$, $K_2 = 0.2137$, and $K_0 = 87.119$. The predicted wind velocity and the ambient temperature for the eighth day are 15.6429 km/h and 47.12706 °C, respectively. Using (5), the tank temperature is calculated and is 50.351°C. It is assumed that the tank temperatures of the two power transformers in the microgrid are the same since they are in close vicinity in the microgrid. Otherwise, if the local data at both places are available, then the two tank temperatures can be computed for the eighth day using the same procedure for the particular hour.

TABLE III
CONSTANTS IN (4)

S.NO	Constants	Wind Velocity	Ambient Temperature
1.	A_1	-5.01924	-3.002052
2.	A_2	-1.2548	-0.5500104
3.	A_3	2.50962	0.3833971
4.	A_4	1.2548	-2.183473
5.	A_5	-2.00769	2.483564
6.	A_6	-2.5096	-2.0667976
7.	A_7	2.0076	4.9337588

B. Generation Power Capacity Availability

The proposed composite power system consists of a conventional generating unit and a wind generator. Both

are connected to the network through power transformers. The power transformer rating is not constant and it depends on the tank temperature. Hence, the rating changes from its nominal value and there is a need to know the derating factor of the power transformer. The power injected into the grid is limited to the derated capacity of the interconnecting transformer. Periodical maintenance and continuous monitoring are important for power transformers for better operation. The failure of power transformers leads to financial loss and replacement cost and require large downtime. Complete power outage will occur in the associate transmission and distribution systems due to power transformer failures. The failure may be due to overloading. Hence, the prediction of available transformer capacity is required to control the load. The available capacity of the power transformer is affected by the variation of tank temperature, which depends on ambient temperature, wind velocity, and top oil temperature. The top oil temperature is fixed at 80 ° considering the life of insulation. There will be accelerated dissociation of the oil beyond this temperature [16], [17]. The I^2R losses are more predominant and responsible for the rise in oil temperature compared with other losses, which are small in comparison and depend on voltage and frequency, which are fairly constant. Transformer I^2R losses depend on the connected load. Thus, the difference between top oil temperature (80°) and the tank temperature decides permissible amount of I^2R losses, which in turn leads to the permissible rating of the transformer [14]–[16]. The difference in temperature ΔT decides the permissible value of load connected and the derating factor the transformer capacity

$$\Delta T = C[I^2R] \tag{6}$$

where C depends on the thermal resistance of oil. Both C and R (Transformer winding resistance) are assumed to be constant for a given transformer and I is the RMS value of the load current.

Therefore

$$I = \sqrt{\frac{\Delta T}{\mathrm{CR}}} \tag{7}$$

and

$$\text{Power Transformer Rating} = (\text{Votage} \times \text{Current})\alpha\sqrt{\Delta T}. \tag{8}$$

The derating factor is proportional to the RMS rating of the current. The distortion in the current waveform expressed in terms of Total Harmonic Distortion (THD) due to nonlinear loads increases the RMS value and so the losses for the same fundamental current. Therefore, for the same tank temperature, the permissible RMS current magnitude should be decreased to maintain the prescribed top oil temperature. Therefore, the derating factor decreases with the increase in THD.

The tank temperature of the eighth day is predicted based on past one-week hourly data and the rating of the transformer is mostly affected by the losses. The major parts of the losses in a power transformer are from the copper windings (i.e., heat losses or I^2R losses) and remaining losses are much less compared with I^2R losses. The transformer top oil temperature changes due to the load variations and the ambient temperatures. As a result, the heat losses go up during heavy loaded situations and increase the temperature difference between the top oil and the tank. This will affect the rating of the transformer. In this paper, only the I^2R losses are assumed to affect the difference in temperatures of tank and top oil, and thereby, the rating of the transformer is given by (8). The derating factor is developed based on the above-mentioned analysis. The derating factor and the available megavolt-ampere rating of the transformer are obtained as given in (9)

$$K = \sqrt{\frac{\text{Difference between } T_{\text{top oil}} \text{ and } T_{\text{tank}}}{\text{Difference between the nominal } T_{\text{top oil}} \text{ and } T_{\text{tank}}}}$$

where $T_{\text{top oil}}$ is the top oil temperature and T_{tank} is the tank temperature

$$K = \sqrt{\frac{\Delta \mathrm{T}}{\Delta \mathrm{T}_{\mathrm{Nominal}}}} = \frac{I_{\mathrm{Permissible}}}{I_{\mathrm{Nominal}}} = \frac{\text{New Rating}}{\text{Nominal Rating}}$$

$$\text{Available MVA rating of transformer} = K \times \text{Nominal rating of transformer.} \tag{9}$$

The nominal oil temperature and tank temperature of the transformer are 80 °C and 45 °C, respectively. The power transformer at conventional generation of a nominal rating of 5 MVA and an average load of 4 MW 0.8 power factor (5 MVA) and the power transformer at the wind farm side of a nominal rating of 5 MVA are considered to have the same derating factor. The derating factor for the particular hour in each day is shown in Table IV. The wind generating unit capacity variations are also considered for analysis. If the nominal capacity of wind generator is 5 MVA at a nominal wind velocity (V_o) of 15 km/h, the new rating on the eighth day is given by

$$\text{New Rating on 8th day} = \text{Nominal power capacity} \times \left(\frac{\text{Velocity on 8th day}}{\text{Nominal Velocity}}\right)^3. \tag{10}$$

The extractable wind power by the wind turbine depends on its design parameters, wind velocity, and air density. Therefore, the available wind power from the same wind turbine is a

TABLE IV
DERATING FACTOR FOR EACH DAY

Day No	Tank Temperature (℃)	De-rating Factor (K)	New Rating of the Transformer 1 (MVA) (connected to the conventional generator)	New Rating of the Transformer 2 (MVA) (connected to the wind farm)
1.	55.0	0.8451	4.2255	4.2255
2.	52.4	0.8880	4.4400	4.4400
3.	48.2	0.9531	4.7650	4.7650
4.	49.5	0.9335	4.6675	4.6675
5.	53.6	0.8684	4.3420	4.3420
6.	47.8	0.9591	4.7955	4.7955
7.	51.2	0.9071	4.5355	4.5355

TABLE V
WIND POWER GENERATED FOR EACH DAY

S. No	Day	Wind Velocity (km/hour)	Power Generated in Wind Plant (MVA)	Net power available from wind farm
1	Mon	13.5	3.6	3.6000
2	Tue	15.0	5	4.4400
3	Wed	16.5	5 (6.65)	4.7650
4	Thus	16.0	5 (6.06)	4.6675
5	Fri	14.7	4.7	4.3420
6	Sat	16.5	5 (6.65)	4.7955
7	Sun	16.3	5 (5.43)	4.5355

TABLE VI
AVERAGE AND ACTUAL POWER AVAILABILITY AT LOADS

S.NO	Load	Probability of Average Power availability Eq (1)	Probability of available Power capacity at each load Eq (11)	Power Capacity available MVA Eq (12)
1.	Load 1	0.97800	0.28613	2.6352
2.	Load 2	0.85816	0.25107	2.3123
3.	Load 3	0.62317	0.18378	1.6926
4.	Load 4	0.95360	0.27899	2.5694

function of wind velocity and air density. As an approximation, it is generally considered that for the short-term forecasting, the variation in air density need not be considered [5]. Hence, in (10), the power available from the wind generator is assumed to be proportional to the cube of the wind velocity. If the air density data are available, it can be included in the calculation of available wind power.

The wind velocity on the eighth day as computed in Section III-A is 15.64 km/h. Hence, the actual power generating capacity available from the wind farm on the eighth day using (10) is 5.66 MVA. However, the power generation is limited to 5 MVA. The derating factor of the power transformers on the eighth day computed from (9) is 0.9203, which is the same for the both transformers. The power capacity available at the point of connection of power transformers to the grid using the derating factors on the eighth day for the transformer near the conventional generating unit is 4.605 MVA and for the transformer near the wind farm side is 4.605 MVA (G_2). Therefore, the net power capacity available from wind farm is only 4.605 MVA irrespective of wind generating power capacity of 5 MVA. The actual power injected into the network is limited by the permissible rating of the connecting transformer. Similarly, the power injected into the grid from the conventional generation is also restricted to 4.605 MVA due to the reduction in the capacity of its connected power transformer. From this, it is clear that the conventional power injected into the grid is affected by only the tank temperature of the power transformer connected to it. The derated capacities of the power transformers connected to the conventional unit and the wind generation unit over the past one week are given in columns 4 and 5 of Table IV. The power delivered to the grid by the conventional unit is the same as given in column 4 of Table IV.

The wind power generation is affected by the wind velocity as well as the tank temperature of the connected power transformer. The power generated from the wind generation for the particular hour is shown in column 4 of Table V. The wind velocities on some days at the specified hour are more than the rated velocity. During these days, the wind generation is more than 5 MVA and it is limited to the actual rated power of 5 MVA of the wind generator, which is given in Table V. The derated capacity of the connected transformer is shown in column 5 of Table IV. Therefore, the net power available for the particular hour from the wind farm is constrained by the derated capacity of transformer and is shown in column 5 of Table V. If the wind velocities on some days are less than the rated velocity and the connected power transformer derating is more than the available wind power, then the actual wind power generated will be injected into the grid.

The standard deviation of the power fed into the grid from the wind farm in the particular hour for the past one week is 0.02. The standard deviation for the predicted power fed into the grid by the wind farm is assumed to be same as 0.02 over the hour on the eighth day. The standard deviation of the hourly average power injected by the conventional unit is calculated as 0.01 based on the past one-week data. It is assumed that the predicted power injected into the grid on the eighth day for the particular hour by the conventional unit equal to 4.605 MVA (G_1) will also have the same standard deviation over that hour.

IV. METHODOLOGY

The main objective of this paper is to compute the available power capacity at load bus. The average power availabilities at each load bus are computed from (1) and (2), where equivalent failure and repair rates are computed using the classical node elimination method [28].

If P_1, P_2, P_3, and P_4 are these probabilities, then the probability of availability of power at each consumer bus is given as

$$\text{Probability of power avaliable at load bus} = \frac{P_n}{\sum P_n}. \quad (11)$$

These probabilities at the load buses are given in Table VI. Column 3 gives the probability of average power availability at each load bus and column 4 gives the actual power availability at each load bus is calculated using (11)

$$\text{The power capacity availability at load bus 1} = \frac{P_1}{(P_1+P_2+P_3+P_4)}(G_1+G_2) \quad (12)$$

where G_1 and G_2 are the computed capacities of power available through the transformers from the conventional generator and wind farm for the eighth day. Similarly, the available power capacity on the eighth day can be computed at the other load buses and is shown in column 5 of Table VI.

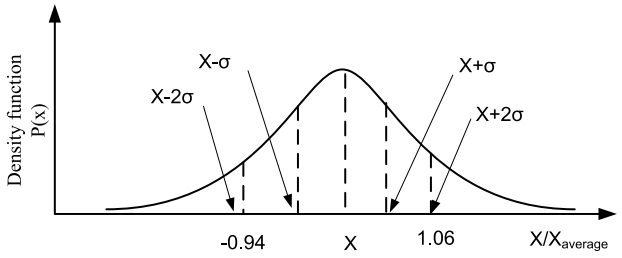

Fig. 4. Normal density distribution function.

TABLE VII
LIMITS ON AVAILABLE POWER CAPACITY AT LOADS

S.NO	Load	Lower limit of available power capacity (MVA)	Upper limit of available power capacity (MVA)
1.	Load 1	2.5297	2.7406
2.	Load 2	2.2198	2.4047
3.	Load 3	1.6248	1.7603
4.	Load 4	2.4666	2.6721

Assuming normal distribution for the available power capacity, its standard deviation is calculated from the available past one-week data for the specified hour. Fig. 4 shows the normal density distribution curve with the mean value of a variable (X/X_{average}) equal to $X_o = 1.0$ and the standard deviation (σ), where X is the actual value. Based on the probability theory for normal distribution, the variable (X/X_{average}) will stay between the limits $(1-2\sigma)$ and $(1+2\sigma)$ with a confidence level of 95%.

In this paper, X_{average} is the predicted available power capacity (Q) at the specified hour on the eighth day. Its standard deviation σ is calculated in Section III from the past seven-day data, which is equal to 0.01 for conventional power generation and 0.02 for the wind power generation. The predicted lower limit of the power available from the conventional power unit (G_1) on the eighth day for the particular hour is 4.51 MVA and the upper limit is 4.69 MVA. Similarly, the lower limit on the power available (G_2) from the wind farm on the eighth day is 4.4208 MVA and the upper limit is 4.7892 MVA. The total power (G) injected into the grid is equal to the sum of G_1 and G_2. The corresponding predicted values of lower and upper limits of the total power available on the eighth day at specified hour at each load bus are given in Table VII.

V. RESULTS AND DISCUSSION

In this paper, the average available power capacity at load bus is calculated. The average power capacity of the proposed composite system is predicted in advance by considering all the possible nonlinearities. The total average power capacity available to the microgrid on the eighth day at the specified hour is 9.21 MVA. Using the methodology followed, the total power capacity available stays between 8.8416 and 9.5784 MVA with a confidence limit of 95%, and average powers available at each load bus on the eighth day are 2.6352, 2.3123, 1.6926, and 2.5694 MVA. From this, the probable limits on the available power capacity at each load with a confidence limit of 95% are given in Table VII.

VI. CONCLUSION

This paper proposes a methodology to evaluate the power capacity availability at different load buses in a composite power system. The generating system nonlinearities are included to estimate the average power availability. In this paper, the power transformer and wind farm power capacity are predicted in advance and used to calculate the available power capacity at each load bus.

APPENDIX

TABLE VIII
STATION NAME: KUTCH–MANDVI (GUJARAT, INDIA)

S.No	Date	Time (UTC)	Latitude (N)	Longitude (E)	Wind Speed (Km/hour)
1.	22-02-2016	3.00.00	22.8	69.3	13
2.	23-02-2016	3.00.00	22.8	69.3	10
3.	24-02-2016	3.00.00	22.8	69.3	12
4.	25-02-2016	3.00.00	22.8	69.3	16
5.	26-02-2016	3.00.00	22.8	69.3	13
6.	27-02-2016	3.00.00	22.8	69.3	18
7.	28-02-2016	3.00.00	22.8	69.3	17
8.	29-02-2016	3.00.00	22.8	69.3	18

The predicted wind velocity on February 29, 2016 is 18.84 km/h by the proposed method.

TABLE IX
STATION NAME: KUTCH-MANDVI (GUJARAT, INDIA)

S.No	Date	Time (UTC)	Latitude (N)	Longitude (E)	Wind Speed (Km/hour)
1.	24-02-2016	1.00.00	22.8	69.3	11
2.	25-02-2016	1.00.00	22.8	69.3	10
3.	26-02-2016	1.00.00	22.8	69.3	12
4.	27-02-2016	1.00.00	22.8	69.3	16
5.	28-02-2016	1.00.00	22.8	69.3	14
6.	29-02-2016	1.00.00	22.8	69.3	15
7.	01-03-2016	1.00.00	22.8	69.3	15
8.	02-03-2016	1.00.00	22.8	69.3	11

The predicted wind velocity on March 2, 2016 is 11.55 km/h by the proposed method.

TABLE X
STATION NAME: RAJPIPLA (GUJARAT, INDIA)

S.No	Date	Time (UTC)	Latitude (N)	Longitude (E)	Temperature (°C)
1.	24-02-2016	1.00.00	21.8	73.5	13.6
2.	25-02-2016	1.00.00	21.8	73.5	20.0
3.	26-02-2016	1.00.00	21.8	73.5	16.1
4.	27-02-2016	1.00.00	21.8	73.5	16.5
5.	28-02-2016	1.00.00	21.8	73.5	18.9
6.	29-02-2016	1.00.00	21.8	73.5	21.2
7.	01-03-2016	1.00.00	21.8	73.5	20.9
8.	02-03-2016	1.00.00	21.8	73.5	22.9

The predicted temperature on March 2, 2016 is 21.9° C by the proposed method.

TABLE XI
STATION NAME: BANGAPET–KOLAR (KARNATAKA, INDIA)

S.No	Date	Time (UTC)	Latitude (N)	Longitude (E)	Temperature (°C)
1.	01-02-2016	9.00.00	12.95	78.26	30.1
2.	02-02-2016	9.00.00	12.95	78.26	29.9
3.	03-02-2016	9.00.00	12.95	78.26	29.0
4.	04-02-2016	9.00.00	12.95	78.26	29..3
5.	05-02-2016	9.00.00	12.95	78.26	26.1
6.	06-02-2016	9.00.00	12.95	78.26	28.3
7.	07-02-2016	9.00.00	12.95	78.26	29.3
8.	08-02-2016	9.00.00	12.95	78.26	29.1

The predicted temperature on February 8, 2016 is 28.49° C by the proposed method.

ACKNOWLEDGMENT

The authors would like to thank MOSDOC, Government of India, for its contribution by providing necessary weather data to conduct this research.

REFERENCES

[1] R. Billinton and R. N. Allan, *Reliability Evaluation of Power Systems*. New York, NY, USA: Plenum, 1996.

[2] R. Karki, P. Hu, and R. Billinton, "Reliability evaluation considering wind and hydro power coordination," *IEEE Trans. Power Syst.*, vol. 25, no. 2, pp. 685–693, May 2010.

[3] R. Billinton, R. Karki, Y. Gao, D. Huang, P. Hu, and W. Wangdee, "Adequacy assessment considerations in wind integrated power systems," *IEEE Trans. Power Syst.*, vol. 27, no. 4, pp. 2297–2305, Nov. 2012.

[4] R. Billinton and G. Bai, "Adequacy evaluation of generation systems including wind energy," in *Proc. IEEE Can. Conf. Elect. Comput. Eng. (CCECE)*, vol. 1. May 2002, pp. 24–29.

[5] R. Billinton, Y. Gao, and R. Karki, "Composite system adequacy assessment incorporating large-scale wind energy conversion systems considering wind speed correlation," *IEEE Trans. Power Syst.*, vol. 24, no. 3, pp. 1375–1382, Aug. 2009.

[6] R. Billinton and G. Bai, "Generating capacity adequacy associated with wind energy," *IEEE Trans. Energy Convers.*, vol. 19, no. 3, pp. 641–646, Sep. 2004.

[7] R. Billinton and Y. Gao, "Multistate wind energy conversion system models for adequacy assessment of generating systems incorporating wind energy," *IEEE Trans. Energy Convers.*, vol. 23, no. 1, pp. 163–170, Mar. 2008.

[8] I. A. Metwally, "Failures, monitoring and new trends of power transformers," *IEEE Potentials*, vol. 30, no. 3, pp. 36–43, May/Jun. 2011.

[9] *Guide for Loading Mineralâ Oil Immersed Transformer*, IEEE Standard C57.91-1995, 1995.

[10] *International Standard Loading Guide for Oil Immersed Power Transformers*, document IEC 354, 1991.

[11] B. C. Lesieutre, W. H. Hagman, and J. L. Kirtley, Jr., "An improved transformer top oil temperature model for use in an on-line monitoring and diagnostic system," *IEEE Trans. Power Del.*, vol. 12, no. 1, pp. 249–256, Jan. 1997.

[12] *Draft Recommended Practice for Performing Temperature Rise Tests on Oil Immersed Power Transformers at Loads Beyond Nameplate Rating*, IEEE Standard PC 57.119, 1996.

[13] J. W. Stahlhut, G. T. Heydt, and N. J. Selover, "A preliminary assessment of the impact of ambient temperature rise on distribution transformer loss of life," *IEEE Trans. Power Del.*, vol. 23, no. 4, pp. 2000–2007, Oct. 2008.

[14] M. K. Pradhan and T. S. Ramu, "On the estimation of elapsed life of oil-immersed power transformers," *IEEE Trans. Power Del.*, vol. 20, no. 3, pp. 1962–1969, Jul. 2005.

[15] *Power Transformers—Part 7: Loading Guide for Oil Immersed Power Transformers*, document IEC 60076-7, 2005.

[16] E. F. Fuchs, D. Yildirim, and W. M. Grady, "Measurement of eddy-current loss coefficient P_{EC-R}, derating of single-phase transformers, and comparison with K-factor approach," *IEEE Trans. Power Del.*, vol. 15, no. 1, pp. 148–154, Jan. 2000.

[17] G. Swift, T. S. Molinski, and W. Lehn, "A fundamental approach to transformer thermal modeling. I. Theory and equivalent circuit," *IEEE Trans. Power Del.*, vol. 16, no. 2, pp. 171–175, Apr. 2001.

[18] S. D. J. McArthur, S. M. Strachan, and G. Jahn, "The design of a multi-agent transformer condition monitoring system," *IEEE Trans. Power Syst.*, vol. 19, no. 4, pp. 1845–1852, Nov. 2004.

[19] X. Zhang and E. Gockenbach, "Asset-management of transformers based on condition monitoring and standard diagnosis," *IEEE Elect. Insul. Mag.*, vol. 24, no. 4, pp. 26–40, Jul./Aug. 2008.

[20] G. K. Frimpong, T. V. Oommen, and R. Asano, "A survey of aging characteristics of cellulose insulation in natural ester and mineral oil," *IEEE Elect. Insul. Mag.*, vol. 27, no. 5, pp. 36–48, Sep. 2011.

[21] P. K. Sen and S. Pansuwan, "Overloading and loss-of-life assessment guidelines of oil-cooled transformers," in *Proc. Rural Elect. Power Conf.*, Apr. 2001, pp. B4-1–B4-8.

[22] D. Yildirim and E. F. Fuchs, "Measured transformer derating and comparison with harmonic loss factor (F_{HL}) approach," *IEEE Trans. Power Del.*, vol. 15, no. 1, pp. 186–191, Jan. 2000.

[23] O. E. Gouda, G. M. Amer, and W. A. A. Salem, "Predicting transformer temperature rise and loss of life in the presence of harmonic load currents," *Ain Shams Eng. J.*, vol. 3, no. 2, pp. 113–121, 2012.

[24] C. Wan, Z. Xu, P. Pinson, Z. Y. Dong, and K. P. Wong, "Probabilistic forecasting of wind power generation using extreme learning machine," *IEEE Trans. Power Syst.*, vol. 29, no. 3, pp. 1033–1044, May 2014.

[25] R. Billinton *et al.*, "A reliability test system for educational purposes-basic data," *IEEE Trans. Power Syst.*, vol. 4, no. 3, pp. 1238–1244, Aug. 1989.

[26] H. Bludszuweit, J. A. Dominguez-Navarro, and A. Llombart, "Statistical analysis of wind power forecast error," *IEEE Trans. Power Syst.*, vol. 23, no. 3, pp. 983–991, Aug. 2008.

[27] J. C. Smith, M. R. Milligan, E. A. DeMeo, and B. Parsons, "Utility wind integration and operating impact state of the art," *IEEE Trans. Power Syst.*, vol. 22, no. 3, pp. 900–908, Aug. 2007.

[28] T. Bharath Kumar, O.Chandra Sekhar, and M. Ramamoorty, "Reliability modelling of power system components through electrical circuit approach," *J. Elect. Eng.*, vol. 16, no. 3, pp. 232–239, Sep. 2016.

[29] T. Bharath Kumar, O.Chandra Sekhar, and M. Ramamoorty, "Evaluation of loss of load expected in an integrated energy system," *J. Elect. Eng.*, vol. 16, no. 4, 2016.
[30] J. W. Kolar *et al.*, "Conceptualization and multiobjective optimization of the electric system of an airborne wind turbine," *IEEE J. Emerg. Sel. Topics Power Electron.*, vol. 1, no. 2, pp. 73–103, Jun. 2013.
[31] D. Boroyevich, I. Cvetkovic, R. Burgos, and D. Dong, "Intergrid: A future electronic energy network?" *IEEE J. Emerg. Sel. Topics Power Electron.*, vol. 1, no. 3, pp. 127–138, Sep. 2013.
[32] J. Han, S. K. Solanki, and J. Solanki, "Coordinated predictive control of a wind/battery microgrid system," *IEEE J. Emerg. Sel. Topics Power Electron.*, vol. 1, no. 4, pp. 296–305, Dec. 2013.
[33] M. Fatu, F. Blaabjerg, and I. Boldea, "Grid to standalone transition motion-sensorless dual-inverter control of PMSG with asymmetrical grid voltage sags and harmonics filtering," *IEEE Trans. Power Electron.*, vol. 29, no. 7, pp. 3463–3472, Jul. 2014.

T. Bharath Kumar was born in Guntur, India, in 1991. He is currently pursuing the Ph.D. degree with the Department of Electrical and Electronics Engineering, K L University, Vijayawada, India.

His current research interests include power system reliability, smart grids, renewable energy sources, wind technologies, and the application of AI techniques to power systems.

O. Chandra Sekhar is currently a Professor and the Head of the Department of Electrical and Electronics Engineering, K L University, Vijayawada, India. His current research interests include multilevel inverters, FACTS controllers, microgrids, and smart grids.

Dr. Sekhar was a recipient of the Prestigious Young Scientist Award from SERB/DST.

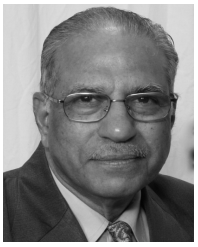

M. Ramamoorty (M'67–SM'72–F'88–LF'06) was a Common Wealth Fellow with the University of Toronto, Toronto, ON, Canada, a Professor with the Department of Electrical Engineering, IIT Kanpur, Kanpur, India, the Chief of Research with ABB Ltd., Vadodara, Gujarat, the Director General of CPRI Bangalore, Bangalore, India, and the Director of ERDA Vadodara, Vadodara. He is currently the Chancellor of K L University, Vijayawada, India, and a Distinguished Visiting Professor with the Department of Electrical Engineering, IIT Kanpur. His current research interests include the applications of power electronics in utilities and industries, power system protection, electrical machines, power quality improvement, and fault detection in machines.

Dr. Ramamoorty is a fellow of INAE, India, and a Distinguished IEEE Lecturer.

S. V. N. L. Lalitha (M'07–SM'16) is currently a Professor with the Department of Electrical and Electronics Engineering, K L University, Vijayawada, India. Her current research interests include power system restructuring and deregulation, transmission pricing in electricity market, and AI and meta heuristics techniques application.